HOW2POWER TODAY
Your Power Design Newsletter

Focus on Magnetics
Sponsored by Payton Planar

ISSUE: April 2024

Designing An Open-Source Power Inverter (Part 17): Transformer Winding Design For the Battery Converter—Alternative Configurations

by Dennis Feucht, Innovatia Laboratories, Cayo, Belize

This latest installment in the Volksinverter design series[1-16] takes the winding design procedure and formulas from part 16 and applies them to winding configurations in search of the optimal winding plan. This represents another aspect of the electrical design of the transformer for the boost push-pull (BPP) power-transfer circuit employed in the battery converter stage of the Volksinverter (Figs. 1 and 2).

The winding sequence is primary first (onto the center-leg of the core), secondary last (exposed to ambient). In general, all windings of the input current polarity are primary and all windings of opposing output currents are similarly lumped together as the secondary winding(s). The Volksinverter has two identical primary windings and only one secondary winding.

In part 12 we determined that the turns ratio n = 1/4, and in part 15, that the primary turns N_p = 6. Thus N_s = N_p /n = 24. In part 16 the winding geometric configuration (sequential) and allotment of winding areas in the window were determined, and given the turns, the maximum bundle sizes. We also need to consider eddy-current resistance ratios in winding design plans, which we'll do here.

An additional and unusual consideration applicable to high-current, low-voltage (or low-R_g) design is the large size of the primary winding bundles. A winding bundle of one wire is a single-strand or N_s = 1, and turns are bundle turns N_b. As bundle diameters become a significant fraction of the allotted winding area width w_w and height h_w, these dimensions have a significant boundary effect on packing factor k_p.

The transformer of a low-R_g power-transfer circuit has a few primary turns of large size, and this brings the winding aspect ratio a_w = w_w/h_w into consideration because wires with diameters that are integer multiples of the allotted winding-area width and height fill it, maximizing conductor area and fill factor and minimizing static R_w, or R_{w0}.

With large bundle radius r_{bw}, a_w becomes a significant geometric parameter affecting winding design. This is not as relevant for high-R_g designs such as off-grid supplies that have many turns of small wire, but is significant for the low-R_g battery converter. Consequently, we examine the wire size fit for the given winding area dimensions.

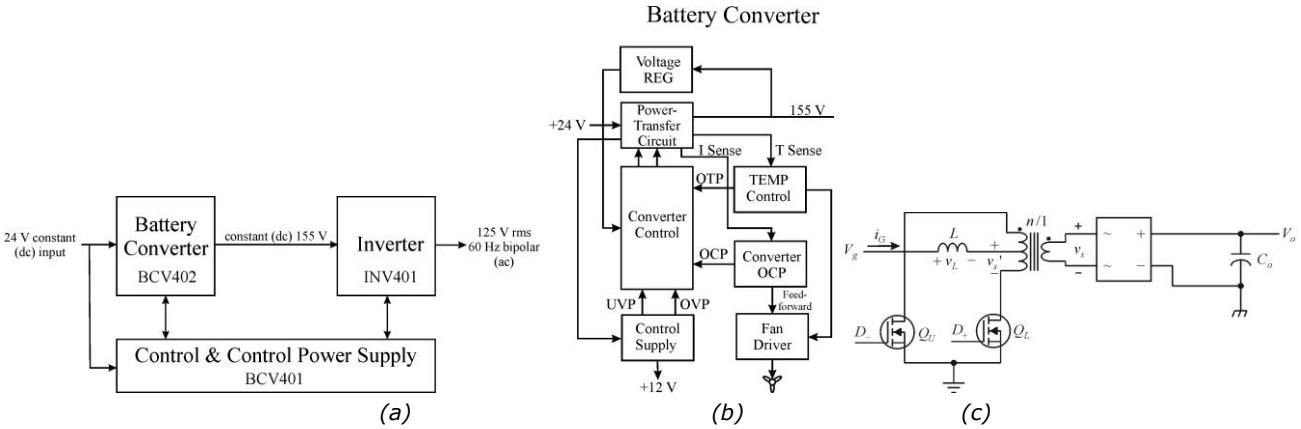

Fig. 1. The Volksinverter's system block diagram (a), the BCV402 battery converter stage block diagram (b) and the CA (boost) push-pull power-transfer circuit (BPP) (c).

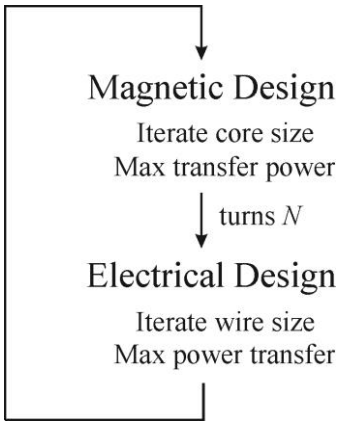

Fig. 2. General procedure for transductor (multi-winding magnetic component) designs.

Maximum Static Winding And Bundle Area Allocations

The winding area allocation of part 16 led to the maximum possible primary winding current $\tilde{i}_p$ and maximum sizes of turns bundles. From the core catalog the ETD34 geometric parameters are

$$V = 7.64\ \text{cm}^3;\ A = 97.1\ \text{mm}^2;\ A_w = 123\ \text{mm}^2;\ w_w = 20.9\ \text{mm};\ h_w = 6.0\ \text{mm} \Rightarrow a_w = 3.5$$

Given the winding area allocations from part 16, the ETD34-3C90 winding areas and dimensions for bobbin (coil-former) window area A_w are

Primary windings $A_{wp} = k_{wp} \cdot A_w = (0.6) \cdot (123\ \text{mm}^2) = 73.8\ \text{mm}^2$; $w_{wp} = w_w = 20.9$ mm ; $h_{wp} = (0.6) \cdot 6.0$ mm $= 3.6$ mm

Secondary winding $A_{ws} = k_{ws} \cdot A_w = (0.4) \cdot (123\ \text{mm}^2) = 49.2\ \text{mm}^2$;
$w_{ws} = w_w = 20.9$ mm; $h_{ws} = (0.4) \cdot 6.0$ mm $= 2.4$ mm

Worst-case square packing (turns aligned between layers) has $k_{pf} = \pi/4 \approx 0.7854$. Then

Primary packed winding area = $A_{wp} \approx k_{wp} \cdot A_w \cdot k_{pf} = (0.6) \cdot (123\,\text{mm}^2) \cdot (0.7854) = 57.96\,\text{mm}^2$

Secondary packed winding area = $A_{ws} \approx k_{ws} \cdot A_w \cdot k_{pf} = (0.4) \cdot (123\,\text{mm}^2) \cdot (0.7854) = 38.64\,\text{mm}^2$

The allowable bundle radius is found from the maximum area:

Primary winding turns bundle area = $A_{bwp} = \dfrac{A_{wp}/2}{N_p} \approx \dfrac{57.96\,\text{mm}^2/2}{6} = 4.83\,\text{mm}^2$

$\Rightarrow r_{bwp}' = \sqrt{\dfrac{A_{bwp}}{\pi}} \approx 1.24$ mm (for #11 AWG)

A bundle of primary winding strands has a twisted (') radius of r_{bwp}'. One-strand bundles are large (untwisted) wires.

Secondary winding turns bundle area = $A_{bws} = \dfrac{A_{ws}}{N_s} \approx \dfrac{38.64\,\text{mm}^2}{24} = 1.61\,\text{mm}^2$

$\Rightarrow r_{bws}' = \sqrt{\dfrac{A_{bws}}{\pi}} \approx 0.716$ mm (for #16 AWG)

These primary and secondary insulated-wire (*w* subscript) bundle radii r_{bw}' are the estimated maximum size, whether as a twisted bundle (r_{bw}') or untwisted single strand (r_{bw}), based on $k_p < k_{pf}$ and including porosity but without winding-area boundary or eddy-current effects. These r_{bw}' values set an upper bound on bundle size.

Bundle Length

The pertinent dimensions of the ETD34 bobbin are r_i = 6.7 mm, r_o = 12.7 mm, and h_w = 6.0 mm. The average radii for primary and secondary winding turns and winding lengths based on these radii are

$$\bar{r}_p = r_i + \frac{(0.6)\cdot h_w}{2} = 8.5 \text{ mm};\ l_{wp}' = l_{wp}/k_{tw} = (2\cdot\pi\cdot\bar{r}_p\cdot N_p + M_p\cdot(w_w/2))/k_{tw} = 32.70 \text{ cm} + (1.066 \text{ cm})\cdot M_p$$

$$\bar{r}_s = r_o - \frac{(0.4)\cdot h_w}{2} = 11.5 \text{ mm};\ l_{ws}' = l_{ws}/k_{tw} = (2\cdot\pi\cdot\bar{r}_s\cdot N_s + M_s\cdot w_w)/k_{tw} = 176.95 \text{ cm} + (2.133 \text{ cm})\cdot M_s$$

Twisting increases bundle radius, reducing bundle packing factor by k_{tw}, a number that depends on the twist pitch length p per twisted bundle radius r_b'.[17] A value of k_{tw} = 0.98 corresponds to a bundle twist pitch $p = 30\cdot r_b$' where twisted bundle outer radius $r_{bw}' = r_b' + r_{cw}$; r_b' is the twisted bundle radius to the center of the outermost bundle strand. This value of $p/r_b' = 30$ is a typical "tightness" of twist, although it has been derived elsewhere (see the note below) that an "optimal" maximum $p/r_b' = 2\cdot\pi \approx 6.28$. A few centimeters are added for lead length and to cover any equation error.

(Note: In reference [17], $p = 2\cdot\pi\cdot r_{bw}$' is given as *optimal* only in that it expresses a *minimum* practical value for p. The breakpoint at $2\cdot\pi$ is asymptotic with an actual value of twisted bundle pitch that approaches that of an untwisted bundle. Consequently, this "optimum" is the value of pitch where any greater twisting (smaller p) becomes highly suboptimal. Typical values of p in the range of 20 to 30 stay well away from this breakpoint and do not significantly affect bundle length and diameter while providing nulling of the interbundle proximity-effect. The $2\cdot\pi$ value is *optimal* as a tradeoff between bundle expansion and proximity-effect nullification.)

Eddy-Current Effects

On the Fig. 3 eddy-current graph of F_r from reference [18], repeated here as Fig. 3, both #11 and #16 AWG wires are in the high-ξ_r region of decreasing F_r with increasing wire size. This is wire large enough for the skin-effect to overcome and dominate the proximity-effect by increased skin-depth surface conduction area.

A high-ξ_r solution of large wire has minimum *bundle* F_r of $f_r = F_r/N_s$ at #9 AWG on the Fig. 4 graph (or at $\xi_{rA\text{med}}$ more generally). However, f_{rA} settles in Fig. 4 to a relatively high value ($f_{rA\text{med}} \approx 0.5$ in Fig. 4 for $\xi_{rA} > \xi_{rA\text{med}}$ or 9 AWG) and is usually too high. Consequently, bundle areas are divided into multiple strands ($N_s > 1$) of smaller wire.

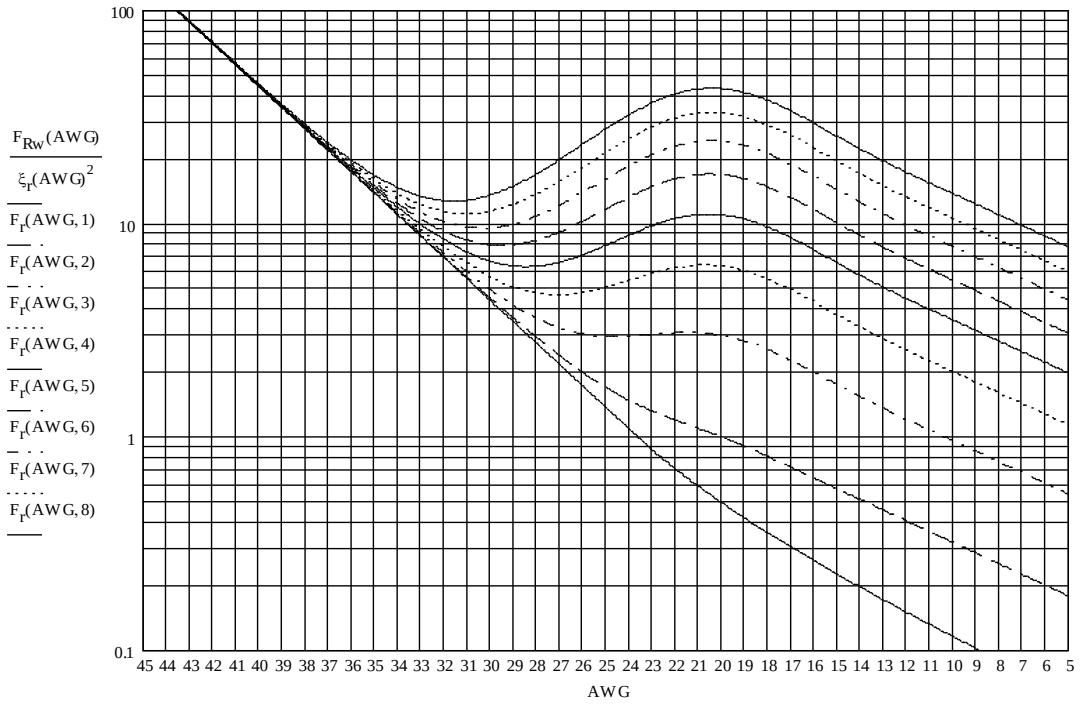

Fig. 3. Eddy-current resistance-ratio F_r at magnetic f = 75 kHz and $R_{\delta r}/l_w$ = 94.2 mΩ/m for Cu at 80°C. F_r(AWG, M) has winding layers M. The lowest plot F_{rw} is that of a single, isolated wire (no proximity effect). The proximity effect dominates over the skin effect where the plots rise, between ξ_{rv} and ξ_{rp}, for M ≥ 2.

Given a winding bundle area allotment, the choice of a magnetic operating-point (op-pt) is along the constant-area red curves of f_{rA} in Figs. 4 and 5 for eddy-current loss within a bundle of N_s > 5 strands. The magnetic op-pt can be shifted to a desired f_{rA} value by maintaining constant bundle size while varying strand size and strands N_s.

The graph of Fig. 4 is f_r (AWG, M_x) = F_r/N_s at magnetic frequency f = 75 kHz for N_s untwisted strands; M_x varies with wire size ξ_r (in units of skin depth δ) depending on which constraint x is applied to the winding. The familiar plots of Dowell's equation $F_r(\xi_r, M)$ found in magnetics textbooks hold M constant as a parameter. M need not be inserted as a constant into Dowell's equation but can vary as a function of winding geometry that holds as constant winding area A_{ww} or N_s as M varies as depicted in Fig. 4.

The plots of Figs. 3, 4 and 5 are based on the Dowell-equation winding model: single untwisted turns of unbundled strands in layers. When applied to within a twisted bundle for N_s > 5 they include the intrabundle (internal) proximity-effect and the strand skin-effect, but the interbundle (external) proximity-effect (according to the rules in reference [18]) is eliminated by twisting.

The skin depth for 80°C Cu wire at f = 75 kHz is

$$\delta_{Cu} = \frac{73.5\,\text{mm}}{\sqrt{f\,/\text{Hz}}},\ 80\ °\text{C, Cu} \ \Rightarrow\ \boxed{\delta_{Cu}(75\ \text{kHz}) = 0.2684\ \text{mm}}$$

Constant f results in constant δ, and $\xi_r = r_c/\delta(f)$ becomes wire size in units of δ and varies only with wire conductive radius r_c. Then for magnetics driven by constant frequency f, a measure of wire size is ξ_r.

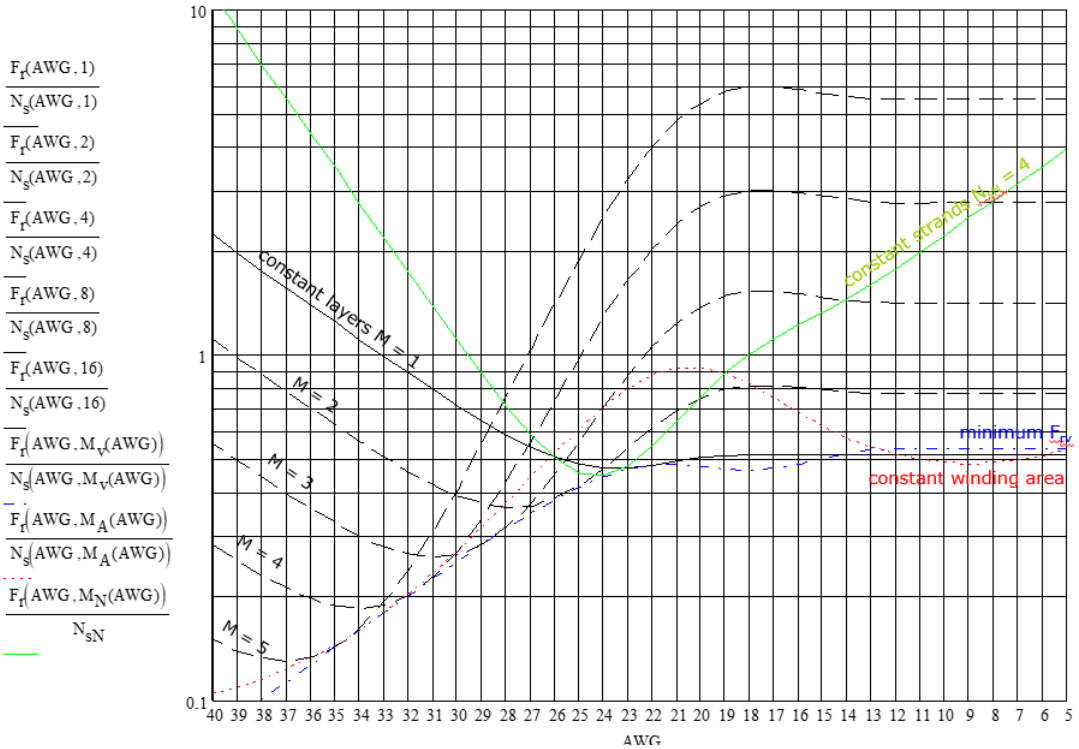

Fig. 4. ETD34 primary winding $f_r = F_r/N_s$ plots: minimum F_{rv} (blue, dash-dot), constant winding area (red, dot), constant strands $N_{sN} = 4$ (green, solid), and constant layers M (black, dash). M = 1 plot is solid black; f = 75 kHz.

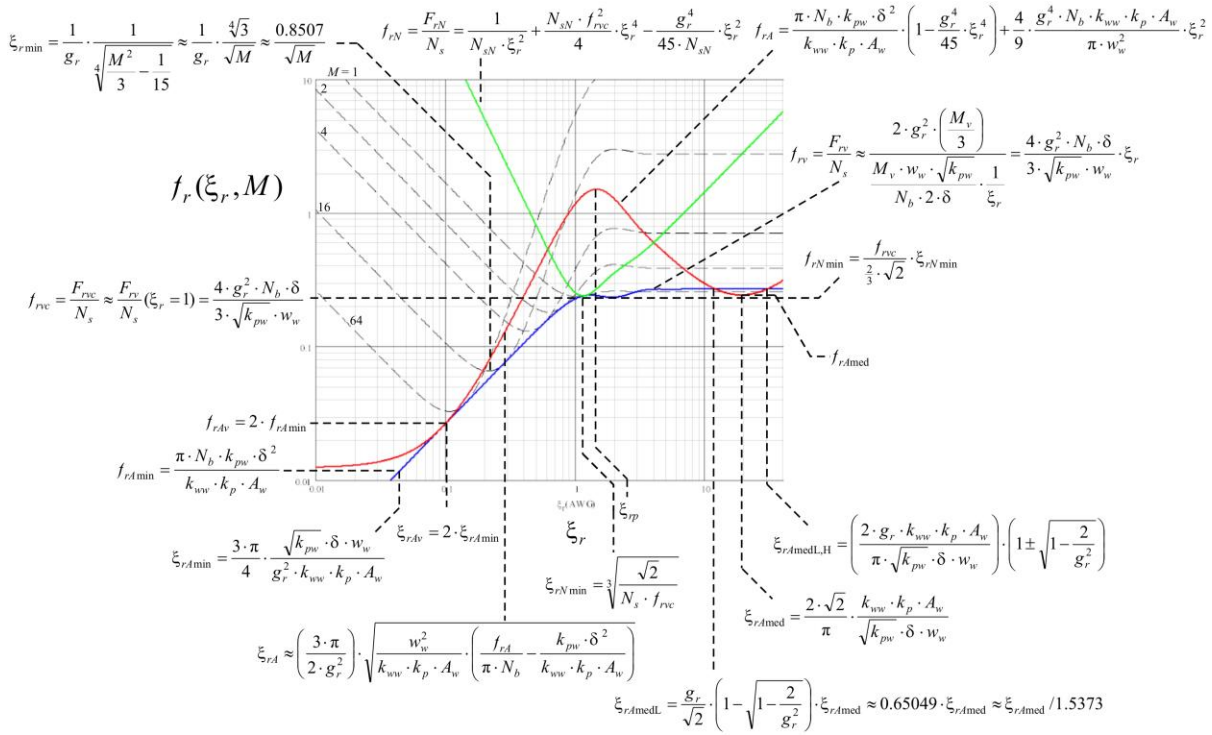

Fig. 5. Operating-points of wire size ξ_r plotted for untwisted bundle resistance-ratio $f_r(\xi_r, M)$ with design formulas.

Primary Windings

We now consider primary winding plans of twisted winding configurations at alternative magnetic op-pts. The large-wire solution at ξ_{rmed} (Fig. 5) shows a boundary-effect impracticality that constrains filling the area with conductor. The smallest wire, at ξ_{rAmin}, is calculated to place a lower bound on strand size range for in-house winding construction.

If $f_{rAmin} < f_{ropt}$, then a third op-pt of interest is at wire size ξ_{rAv} where winding area is fit by wire size and eddy-current loss is at a minimum. The fourth option for more than five bundle strands is to calculate the optimal strand size that minimizes the intrabundle eddy-current effect within the winding area constraint.

The op-pt strand sizes can be found from the Dowell-equation algebraic approximations given in part 16 (or Fig. 5) or by graphically plotting them from the Dowell equation. What follows are design plans demonstrative of the essential concepts and design procedure.

Plans for the primary windings have configurations that maximize k_p for the given wire size. Eddy-current formulas for selected op-pts result in R_{wp} and are compared to the R_{wp} goal of R_{wpopt}. Plans vary in how the bundle turns are configured in the given winding area and also in the number of strands in the bundle(s). The large bundle size of high-ampacity primary windings relative to their winding area dimensions presents an additional geometric design constraint that is considered first.

Aspect Ratios And Winding Configuration

The boundary effect of allotted winding area dimensions on large wire reduces packing factor k_p. The best fit of round wire or bundle layers is for both winding width w_w and height h_w to be an integer multiple of wire or bundle diameter. For each winding area, aspect ratio $a_{wx} = w_{wx}/h_{wx}$ is ideally an integer. (In this expression, x can represent a primary (either one) or secondary winding.)

The combined window dimensions for Volksinverter ETD34 primary windings are w_w = 20.9 mm and $k_{wp} \cdot h_w$ = (0.6)·6.0 mm = 3.6 mm. The two primary windings can either be layered along the height or configured side by side along the width. The aspect ratio for the total primary winding area is

$$a_{wp} = \frac{w_{wp}}{h_{wp}} = \frac{w_w}{(0.6) \cdot h_w} \frac{20.9\,\text{mm}}{3.6\,\text{mm}} = 5.81$$

Because a_{wp} is slightly less than 6, round bundles must compress along the width in a "squash fit". Compression does not change k_p, only bundle shape, trading off reduced width for increased height.[19] However, width compression is impractical in construction. Six turns of somewhat smaller round bundles without compression fit the width, leaving some unused length in both the width and height dimensions. The area for both primary windings must accommodate a total of $2 \cdot N_p$ = 12 turns. Six turns fitting the width requires that both primary windings be wound together in a single bundle of one layer, or bifilar-wound.

The aspect ratio for round bundles results in a 6 × 1 or 12 × 2 layer configuration. Separate primary windings can be configured, each with a width fit of six bundles stacked in two layers, as shown in Fig. 6. There are four primary windings in all, paired by layers to double winding ampacity for each of the two primary windings.

Each upper layer of each dotted half-area in Fig. 6 is a winding connected in parallel with the winding beneath it. Both have six turns, as required of N_p and current capacity in parallel doubles. Parallel windings overcome area underutilization from aspect-ratio misfits.

Another way is to twist the strands of the two primary windings in parallel (multifilar) instead of sequential, configuring a single 6 × 1 bundle of an even number of strands, half for each primary winding, that reaches across the full winding area width in six turns. (This will be discussed later in the article.) But first, we proceed to plans of the Fig. 6 scheme.

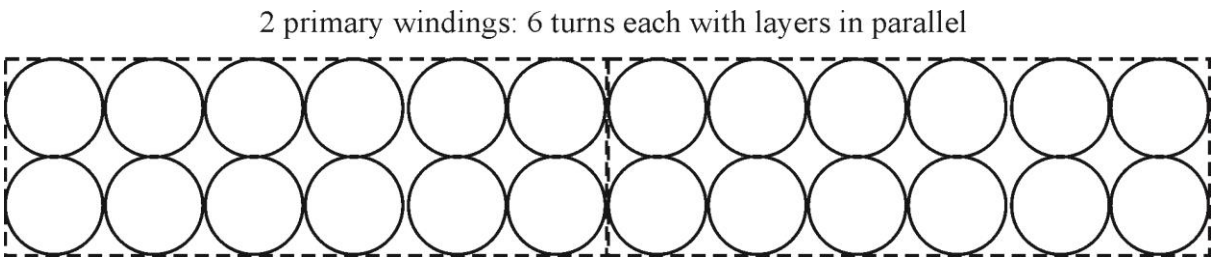

Fig. 6. In a 12 × 2 layer primary winding area, the dotted areas are for each of two primary windings. Each has two parallel windings of one winding per layer of six turns connected electrically in parallel for twice the ampacity.

Plan 1: Primary Large-Wire Plan

In plan 1 the primary windings are single strands of large wire (with no bundling or twisting) that operate in the high-ξ_r skin-effect region of the F_r plots. Turns of both primary windings are shown in Fig. 6. Six turns are fit to a half-width (20.9 mm/2 = 10.45 mm) in two layers per winding, resulting in a wire size of

$$r_{bw} = \tfrac{1}{2}\cdot(10.45\text{ mm})/6 = 0.871\text{ mm} \rightarrow r_{bw}(\#14) = 0.874\text{ mm}$$

Then for two layers, the height is $4\cdot r_{bw}(\#14) = 3.50$ mm < $(0.6)\cdot h_w = 3.6$ mm and two layers fit with 0.1-mm spacing.

By fitting two layers, one layer per winding, to the height instead, the maximum wire size that fits is

$$r_{bw} = \tfrac{1}{2}\cdot\frac{h_{wp}}{2} = (3.6\text{ mm})/4 = 0.9\text{ mm} \rightarrow r_{bw}(\#14) = 0.874\text{ mm}$$

The width of both layers having N_p turns per layer is $6\cdot(2\cdot 0.874\text{ mm}) = 10.49\text{ mm} = (0.502)\cdot w_w = (0.502)\cdot(20.9\text{ mm})$—a slight compression fit. To fit with smaller wire moves the op-pt on the eddy-current graphs to the left toward the proximity-effect region and increases F_r. Such a plan differs from plan 1 which attempts to achieve a high-ξ_r region op-pt that is optimal at a wire size of $\xi_{rA\text{med}}$.

In general, the aspect ratio of large (high-ξ_r) wire, winding dimensions, and N_p do not lead to a good fit, and the winding design is driven to smaller wire having a size that for both width and height are common integer multiples. In plan 1, a single strand only moderately reduces F_r in its high-ξ_r region; larger wire leads to lower F_r. Yet the larger wire is less compatible with winding aspect ratio, and boundary effects defeat plan 1. It has no options for paralleled or multifilar windings.

Plan 2: Very-Low-ξ_r Wire & And Maximum Bundle Strands

Plan 2 is the other extreme of minimum wire size having an op-pt at $\xi_{rA\text{min}}$ (on Fig. 5), a practical minimum strand size with winding loss at minimum bundle resistance ratio $f_r = f_{rA\text{min}}$, where the asymptote of f_{rA} intersects f_{rv} at $\xi_{rA\text{min}}$. Although the Fig. 4 and 5 graphs do not show the continuation of f_{rA} to the left, it approaches an asymptotic minimum of $f_{rA\text{min}}$. By projecting this asymptote to the right, it intersects the $f_r = f_{rv}$ curve of F_r valley values at an ξ_r value labeled $\xi_{rA\text{min}}$. Algebraic approximation[18] derived from the Dowell equation for wire size corresponding to $f_{rA\text{min}}$ is

$$r_{cA\text{min}} = \xi_{rA\text{min}}\cdot\delta = \frac{3\cdot\pi}{4\cdot g_r^2}\cdot\frac{\sqrt{k_{pw}}\cdot\delta^2\cdot w_{wp}}{A_{wp}} \approx (0.9845)\cdot\frac{(0.75)\cdot(0.2684\text{ mm})^2\cdot(10.45\text{ mm})}{(28.98\text{ mm}^2)} = 0.0192\text{ mm} \rightarrow \#46\text{ AWG}$$

At this small wire size, area-fitting is not a design consideration because the wire is so much smaller than the allotted winding dimensions that a diameter or two of wire hardly affects area utilization. Although $\xi_{rA\text{min}}$ results in a manual-wind wire size that achieves minimum R_{wp}, it is often not a practical solution for in-house bundle construction. If $R_{wp} << R_{wpopt}$, then transfer efficiency variation with current, or $\Delta\eta(i_p)$, is excessive. If $R_{wp} > R_{wpopt}$, then winding loss is excessive, power transfer across windings is reduced, and a larger core is

required.

In the very-low-ξ_r region of $\xi_r < \xi_{rA\min}$, wire the strand size of commercial Litz wire is difficult to construct into bundles and goes against the Volksinverter goal of magnetics construction without specialized equipment. (Hence the Innovatia wire table stops at 42 AWG—see the appendix.) For intrepid builders with the requisite agility, the f_r value is

$$f_{rA\min} = \frac{\pi \cdot N_b \cdot \delta^2}{k_{ww} \cdot k_p \cdot A_w} = \frac{(18.85) \cdot (0.2684\,\text{mm})^2}{(28.98\,\text{mm}^2)} = 46.86 \cdot 10^{-3} = 0.04686 \Rightarrow$$

$$R_{wp} = f_r \cdot (R_w / l_w) \cdot l_{wp} \approx (0.04686) \cdot (94.2\ \text{m}\Omega/\text{m}) \cdot (0.35\ \text{m}) = 1.545\ \text{m}\Omega$$

From part 16, maximum ampacity (static current capacity) is $\tilde{i}_p$ = 13.98 A. Then the winding resistance design goal is

$$R_{wpopt} = \frac{\psi \cdot \bar{P}_c / 4}{\tilde{i}_p^{\,2}} = \frac{0.476\,\text{W}}{\tilde{i}_p^{\,2}} \approx \frac{0.476\,\text{W}}{(13.98\,\text{A})^2} = 2.44\,\text{m}\Omega\ > 1.545\ \text{m}\Omega$$

$R_{wp}(\xi_{rA\min}) < R_{wpopt}$, and the winding area is adequate for larger wire. Extrapolating logarithmically from the AWG wire table, the ampacity of #46 wire is $I_{\max}(\#40)/4 \approx 5.75$ mA—that is, 46 – 40 = 6, and at 3 AWG per octave (for cross-sectional area current density), two octaves less gives × ¼. The number of strands needed for $\tilde{i}_p$ ampacity is N_s = 15.31 A/5.75 mA = 2663. This bundle would require many sub-bundles to minimize F_r—tedious and generally infeasible to construct manually and more expensive as commercial Litz wire. The levels of sub-bundles required for N_s = 5 strands per sub-bundle would be $\sqrt[5]{2663} \approx 4.8 \rightarrow 5$ levels, which is possible, but driving us onward to plan 3.

Plan 3: ξ_{rAv} Wire Size Fits Area And has Minimum F_r

The op-pt at $\xi_r = \xi_{rAv}$ is both constrained by area (as ξ_{rA}) for a winding fit and f_r is minimized to f_{rv} as f_{rAv}. This is an optimal op-pt for winding design. (Plans 1 and 2 are included here for the general winding design template.) The bundle f_r minima lie along the blue plots of Figs. 5 (solid plot) and 4 (dot-dash plot), calculated as

$$f_{rv} = \frac{F_{rv}}{N_s} \approx f_{rvc} \cdot \xi_r \ , \xi_r < 1, M \geq 2$$

The f_{rv} plot has a breakpoint where $M \leq 2$ is small enough to avoid significant proximity effect. The algebraic approximation for f_r minima is f_{rv}, at the boundary between the low-ξ_r and medium-ξ_r regions. The ξ_{rAv} op-pt not only meets the winding-area constraint but also is at an F_r minimum of F_{rv} with strand size $r_{cAv} = \xi_{rAv} \cdot \delta$;

$$\xi_{rAv} = \frac{3 \cdot \pi}{2 \cdot g_r^2} \cdot \frac{\sqrt{k_{pw}} \cdot \delta \cdot w_w}{k_{ww} \cdot k_p \cdot A_w} = 2 \cdot \xi_{rA\min} \Rightarrow r_{cAv} = 2 \cdot r_{cA\min} = 2 \cdot (0.0192\ \text{mm}) = 0.0384\ \text{mm} \rightarrow \#40\ \text{AWG}$$

Round-wire conductive radius r_c doubles every 6 AWG. Thus,

$$r_c(\#46 - 6) = r_c(\#40) = 0.041\ \text{mm}$$

From the calculation of $f_{rA\min}$ in plan 2,

$$f_{rAv} = 2 \cdot f_{rA\min} = 2 \cdot (0.04686) = 0.09372 \Rightarrow R_{wp} \approx 2 \cdot (1.545\ \text{m}\Omega) = 3.09\ \text{m}\Omega > 2.44\ \text{m}\Omega$$

The ampacity of #40 AWG wire is 23 mA. Then N_s = 13.98 A/23 mA = 608—still a large number of strands, though #40 wire is barely large enough to not require extraordinary construction methods. The number of levels of sub-bundling of 5 strands per sub-bundle is $\sqrt[5]{608} \approx 3.6 \rightarrow 4$—still challenging, but feasible for manual construction.

The ξ_{rAv} op-pt has twice the resistance of $f_{rA\min}$ at twice the wire radius. It exceeds R_{wpopt} but the op-pt formulas assume untwisted bundling. If the bundle is built of three-strand sub-bundles (three strands pack tightest for N_s < 5), then the number of sub-bundles is $608^{1/3} \approx 8.47$ bundle levels.

Sub-bundles are combined by extending them to a far hook and returning them to the twist drill chuck to form a loop. Then these can similarly be twisted into a new level of three sub-bundles per new sub-bundle so that the number of sub-bundle levels is about $8.47 \rightarrow 9$. Primary winding bundles are tedious to construct this way, leading us to wonder whether fewer strands of larger wire might be admissible though it deviates from the optimality of ξ_{rAv}.

A math-cluttered Fig. 5 summarizes various op-pt alternatives for untwisted wire. The three that were already chosen are at wire sizes of $\xi_{rA\text{med}}$, $\xi_{rA\min}$, and ξ_{rAv}. Others with their algebraic approximations are shown around the Fig. 5 graph and have been derived in previous *How2Power Today* magnetics articles.

The two plots of interest here are the red and blue—the red being the locus of f_r while holding winding area constant (f_{rA}) and the blue corresponding to the valley values of f_{rv} that mark the boundary between the low-ξ_r and medium-ξ_r regions of the Dowell curves. As layers M decrease, these valley points (minima) on F_r or f_r move to the right on descending plots until they disappear (when the rise in F_r from the proximity-effect ceases).

The algebraic approximations of F_{rv} and f_{rv} extrapolate to the right into the medium- and high-ξ_r regions and remain essentially constant at the value of $f_r(\xi_r = 1) = f_{rvc}$. Thus, strand size typically has a range between ξ_{rAv} and ξ_r = 1. For converter transformers, typical op-pts are found where $\xi_r \le 1$.

Plan 4: $\xi_{rAv} \le \xi_{rA} \le 1$

We have been testing op-pt alternatives for untwisted turns of wire (bundled or not) according to favorable op-pt characteristics instead of seeking the value of $\xi_{rA} = \xi_{ropt}$ corresponding to $f_{rA} = f_{ropt}$. Working the problem instead from the goal of R_{wpopt}, we can find $f_{rA}(R_{wpopt})$ as

$$f_{ropt} = \frac{R_{wpopt}}{(R_{\delta r} / l_w) \cdot l_w}$$

where ξ_{rA} is between ξ_{rAv} and ξ_r = 1. The design formula for this range of wire size is along the ascending segment of the f_{rA} curves of Figs. 4 and 5 graphs for loosely twisted round wire, where N_b is the bundle turns (whether strands are bundled or single wires). From reference [18], wire size in ξ_r for a given $f_{rA} = f_{ropt}$ is

$$\xi_{rA} \approx 2 \cdot \sqrt{\frac{w_w^2}{k_p \cdot (k_{ww} \cdot A_w)} \cdot \left(\frac{f_{rA}}{\pi \cdot N_b} - \frac{k_{pw} \cdot \delta^2}{k_p \cdot (k_{ww} \cdot A_w)} \right)}\ , \xi_r < 1$$

Then the strand conductive radius $r_c = \xi_{rA} \cdot \delta$ and wire size in AWG is found as the nearest smaller r_c in the wire table.

For *twisted* bundles, the ξ_{rA} formula applies to the *intrabundle* proximity-effect and strand skin-effect. Because the Dowell equation does not include bundling, the bundle skin-effect is subtracted from f_{ropt}, leaving

$$f_{rA} = f_{ropt} - f_{rSb} = R_{wpopt} / R_{\delta r} - F_{rw}(r_b') \text{ for } N_s > 5$$

where f_{rSb} is the bundle skin-effect resistance ratio,[17] the second term of the

$$\text{Skin-Effect Equation: } f_{rS} = f_{rSs} + f_{rSb} = F_{rw}(\text{strand})/N_s + F_{rw}(\text{bundle}) = F_{rw}(r_c)/N_s + F_{rw}(r_c \cdot \sqrt{N_s})$$

Bundle radius is derived by arranging N_s strands as a square bundle.[17] Then bundle radius varies with $N_s^{1/2}$, and

$$F_{rw}(\text{bundle}) = F_{rw}(r_c \cdot \sqrt{N_s}) = F_{rw}(\text{AWG} - 10 \cdot \log(N_s))$$

Wire size can be expressed in r_c or r_{cw}, ξ_r, or in AWG. F_{rw}(AWG) is found on the Fig. 3 F_{rw} plot. The eddy-current rules for twisted bundles in reference [18] leave only the strand skin-effect for twisted strands $N_s \le 5$, and

$$f_r = f_{rSs} = F_{rw}(r_c)/N_s = F_{rw}(\text{AWG})/N_s$$

At a magnetic frequency of f = 75 kHz, the static resistance $R_{\delta r}$ of a round wire with radius of one skin depth δ per wire length l_w is

$$\frac{R_{\delta r}}{l_w} = \frac{\rho_{\text{Cu}}}{\pi \cdot \delta(f)^2} \approx (1.256\ \text{m}\Omega/\text{m} \cdot \text{kHz}) \cdot f = 94.2\ \text{m}\Omega/\text{m}\ ,\ 80°\text{C},\ 75\ \text{kHz}$$

We seek a solution of R_{wpopt} = 2.44 mΩ corresponding to $f_r \approx f_{ropt}$ from the primary winding ampacity limit. This optimistic (min R_{wp}) f_r goal is thus

$$f_{ropt} = \frac{R_{wpopt}}{(R_{\delta r}/l_w) \cdot l_w} = \frac{2.44\ \text{m}\Omega}{(94.2\ \text{m}\Omega/\text{m}) \cdot (35\ \text{cm})} = \frac{2.44\ \text{m}\Omega}{33.0\ \text{m}\Omega} = 0.074$$

R_{wpopt} varies depending on the maximum $\tilde{i}_p$ for a given wire or bundle size. Hence f_{rpopt} will also vary for each plan.

Twisted Bundles Simplify Winding Design

The simplified eddy-current rules are that all twisted bundles nullify the interbundle proximity-effect, and twisted bundles with strands $N_s \le 5$ also nullify the intrabundle proximity-effect and bundle skin-effect, leaving only the strand skin-effect.[17, 18] The winding design goal is therefore to find winding configurations for Volksinverter high-ampacity primary windings with few strands of wire that can be bundled so that $R_{wp} \approx R_{wpopt}$ and $f_r \approx f_{ropt}$. We now proceed to analyze twisted winding bundle configurations of different strand size and number for both f_{ropt} (R_{wpopt}) and ampacity requirements that fit the allotted winding dimensions.

Plan A: Three-Strand Bundle, Two Parallel Bundle Layers

Instead of applying the previously given magnetic op-pts, let the allotted winding dimensions drive the configuration with a bundle size of 3 to 7 strands fitting the winding area. Each of the two primary windings has 6 × 2 three-strand bundles because they fit the given winding aspect ratio, with six pairs of turns along width $w_w/2$, electrically in parallel in two layers; $a_{hwp} = (w_w/2)/(0.6) \cdot h_w = 2.90 \approx 3 = 6/2$.

A width fit is attempted as in Fig. 6, allotting half the width $w_w/2$ to each primary winding. The maximum twisted (') bundle radius that fits the width for N_s = 3 strands is

$$r_{bw}'(w) = ½ \cdot (w_w/2)/6 = (w_w/2)/12 = (10.45\ \text{mm})/12 = 0.871\ \text{mm}$$

The maximum bundle radius of M = 2 layers that fits the winding height of $(0.6) \cdot h_w = (0.6) \cdot (6.0\ \text{mm}) = 3.6$ mm is

$$r_{bw}'(h) = \tfrac{1}{2}\cdot(0.6)\cdot h_w/M = 0.90 \text{ mm} \Rightarrow\ a_{bw} = r_{bw}'(w)/r_{bw}'(h) = 0.871 \text{ mm}/0.9 \text{ mm} = 0.968 \approx 1 \Rightarrow \text{round}$$

So, the twisted bundle aspect ratio a_{bw} that fits the primary winding area is almost round, and $r_{bw}' \approx 0.90$ mm.

A three-strand bundle has an untwisted bundle packing of $1/k_{pb} = 1.16$.[20] Twisted bundles expand and also extend in length by $1/k_{tw}$, and r_{bw} increases by $1/\sqrt{k_{tw}}$ to r_{bw}'. Twisting expands the bundle by a factor of $1/k_{tw} = 1.022$ for a pitch p-to-bundle radius of $p/r_b' = 30$.[16] (r_b' is the radius to the center of the outermost layer of strands within the bundle; $r_b' = r_{bw}' - r_{cw}$.) The untwisted strand radius for a given twisted r_{bw}' is

$$\text{Pre-twist } r_{cw} = r_{bw}'/\sqrt{N_s/k_{pb}\cdot k_{tw}} = (0.90\,\text{mm})/\sqrt{3\cdot(1.16)\cdot(1.022)} = (0.90 \text{ mm})/1.886 = 0.477 \text{ mm} \Rightarrow \#20$$
$$\Rightarrow r_{cw}(\#\,20) = 0.448 \text{ mm}$$

The twisted-bundle radius r_{bw}' with #20 wire is thus

$$r_{bw}' = r_{cw}\cdot\sqrt{N_s/k_{pb}\cdot k_{tw}} = (0.448 \text{ mm})\cdot(1.886) = 0.845 \text{ mm} \Rightarrow p = 30\cdot(0.845 \text{ mm} - 0.448 \text{ mm}) = 12 \text{ mm}$$

The bundle size is about that of a #14 AWG wire. For two parallel square-packed layers of twisted #20 × 3 bundles, the combined height is

$$h_{wp} = 4\cdot(0.845 \text{ mm}) = 3.38 \text{ mm} = (0.94)\cdot(3.6 \text{ mm}) \Rightarrow \text{tape spacing} = 0.22 \text{ mm} = 8.7 \text{ mils}$$

Only (1 – 0.94) = 6% of allotted winding height h_{wp} is not utilized by wire bundles and provides space for 0.22 mm (8.7 mil) of insulating tape between primary and secondary windings.

The ampacity of this dual three-strand bundle is

$$I_{\max} = 2\cdot[3\cdot I_{\max}(\#\,20)] = 6\cdot(2.37 \text{ A}) = 14.22 \text{ A}$$

Adjusting the winding current thermally for ETD34 core size,

$$\max\ \tilde{i}_p = (\tilde{J}/\tilde{J}_0)\cdot I_{\max} = (0.978)\cdot(14.22 \text{ A}) = \mathbf{13.91\ A}$$

$$R_{wpopt} = \frac{\psi\cdot\bar{P}_c/4}{\tilde{i}_p^{\,2}} = \frac{0.476\,\text{W}}{\tilde{i}_p^{\,2}} \approx \frac{0.476\,\text{W}}{(13.91\,\text{A})^2} = 2.46\,\text{m}\Omega$$

With $N_s = 3 \le 5$, only the strand skin-effect f_{rSs} remains. With two parallel #20 × 3 bundles, each bundle pair has

$$f_{ropt} = \frac{R_{wpopt}}{(R_{\delta r}/l_w)\cdot l_w} = \frac{2.46 \text{ m}\Omega}{(94.2 \text{ m}\Omega/\text{m})\cdot(35 \text{ cm})} = \frac{2.46 \text{ m}\Omega}{33.0 \text{ m}\Omega} = 0.075$$

Reading from the graph of Fig. 3, $F_{rw}(\#20) = 0.5$. With three parallel strands in each of two parallel bundles,

$$f_r = 0.5/3\cdot 2 \approx 0.083 > 0.075$$

The three-strand choice slightly exceeds f_{ropt} by 9.6%. As a magnetic op-pt in Fig. 4, strand f_r is near ξ_{rp}, the worst-case f_r if the bundles were untwisted. Despite the bundle twisting decrease in winding k_p, twisting significantly decreases f_r.

The BPP transfer-circuit maximum input (inductor) current is thus

$$I_g = (1.633)\cdot \tilde{i}_p = (1.633)\cdot(13.91\text{ A}) = \mathbf{22.7\text{ A}}$$

Then static input power is

$$\overline{P}_{g0} = (20\text{ V})\cdot(22.7\text{ A}) = \mathbf{454\text{ W}}$$

The value of $\overline{P}_{g0}$ from part 16[16] is $\overline{P}_{g0}(\max)$ **=** 457 W. This plan has a value that is less by 0.7%. Static analysis results in a transfer power near the maximum "ideal" static value $\overline{P}_{g0}$. Three strands pack together well, increasing fill factor. Twisting increases the winding length a small factor of $1/k_{tw}$ = 1.022 to l_w = 35 cm. The plan is therefore

2 primary windings of 6 turns each of 2 parallel layers of twisted # 20 × 3 with twist pitch p = 12 mm

Plan C: Five-Strand Bundle, Two Parallel Bundle Layers

The maximum N_s with eddy-current loss advantages is five strands. (The discussion of a four-strand plan B is skipped here because it does not pack much better than five strands but is included in the table below.) The procedure for five-strand plan C has the same three-strand bundle dimensional fit. The only difference is that for N_s = 5 the bundle can compress into an elliptical shape with axes fitting radii of

$$r_{bw}'(w) = w_{bw} = \tfrac{1}{2}\cdot 10.45\text{ mm}/6 = 0.871\text{ mm}\ ,\ r_{bw}'(h) = h_{bw} = \tfrac{1}{2}\cdot 3.6\text{ mm}/2 = 0.90$$

The radius of a round twisted bundle with the cross-sectional area of an ellipse fitting the winding aspect ratio is[21]

$$r_{bw}' = \sqrt{w_{bw}'\cdot h_{bw}'} = \sqrt{(0.871\,\text{mm})\cdot(0.90\,\text{mm})} = 0.885\text{ mm}$$

The bundle equivalent radius is nearly the same as for three strands, but because five strands can be compressed, the elliptical average r_{bw}' is used. Five strands can have three configurations: planetary, pentagon, or hexagonal, with an average $1/k_{pb}$ = 1.37 and

$$1/k_{pb}\cdot k_{tw} = 1/(1.37\cdot 1.022) = 1/1.40 \Rightarrow$$

$$r_{cw} = r_{bw}'/\sqrt{N_s/k_{pb}\cdot k_{tw}} = 0.885\text{ mm}/\sqrt{5\cdot(1.40)} = 0.885\text{ mm}/2.646 = 0.335\text{ mm} \Rightarrow \#\,23 \Rightarrow r_{cw} = 0.321\text{ mm} \Rightarrow$$

$$r_{bw}' = (0.321\text{ mm})\cdot(2.646) = 0.849\text{ mm} \Rightarrow h_{wp} = 4\cdot r_{bw}' = 3.4\text{ mm} \Rightarrow \text{tape spacing} = 0.2\text{ mm} \approx 8\text{ mils}$$

$$\text{bundle twist pitch} = p = 30\cdot(0.885\text{ mm} - 0.321\text{ mm}) = 30\cdot(0.564\text{ mm}) = 17\text{ mm}$$

$$\text{primary } I_{\max} = 2\cdot[5\cdot I_{\max}(\#\,23)] = 10\cdot(1.184\text{ A}) = 11.84\text{ A} \Rightarrow$$

$$\max\ \tilde{i}_p = (\tilde{J}/\tilde{J}_0)\cdot I_{\max} = (0.978)\cdot(11.84\text{ A}) = \mathbf{11.58\text{ A}} \Rightarrow I_g = (1.633)\cdot\tilde{i}_p = (1.633)\cdot(11.58\text{ A}) = \mathbf{18.9\text{ A}}$$

$$\overline{P}_{g0} = V_{g\min}\cdot I_g = \mathbf{378\text{ W}} < \overline{P}_{g0}(\max) = 457\text{ W}$$

$$R_{wpopt} = \frac{\psi \cdot \overline{P}_c / 4}{\tilde{i}_p^{\,2}} = \frac{0.476\,\text{W}}{\tilde{i}_p^{\,2}} \approx \frac{0.476\,\text{W}}{(18.9\,\text{A})^2} = 1.33\,\text{m}\Omega$$

$$\text{Per-layer bundle } f_{ropt} = 2 \cdot R_{wpopt} / R_{\delta r} = 2 \cdot (1.33\ \text{m}\Omega / 33.0\ \text{m}\Omega) = 0.081$$

The twisted five-strand bundle has only strand skin-effect:

$$f_{rSs} = F_{rw}(\#23)/5 = 0.88/5 = 0.176 > f_{ropt} = 0.081$$

The five-strand eddy-current loss exceeds f_{ropt} by about 118%. Therefore five strands is a suboptimal solution.

2 primary windings of 6 turns each of 2 parallel layers of twisted # 23 × 5 with twist pitch p = 17 mm

Plan D: Seven-Strand Bundle, Two Parallel Bundle Layers

If the number of strands does not exceed five by much, then sub-bundling can be reduced to simplify bundle construction though it begins to exhibit additional bundle skin-effect and intrabundle proximity-effect losses. The winding area geometry remains the same as does the bundle size of

$$r_{bw}' = \sqrt{w_{bw} \cdot h_{bw}} = 0.885\ \text{mm}$$

The configuration of seven strands collapses to that of a filled hexagon, with the layer-zero center strand having a shorter length and resistance than the twisting first layer. For seven strands, $1/k_{pb}$ = 1.286 and r_{bw}'/r_{cw} = 3.033. Then

$$r_{cw} = r_{bw}' / \sqrt{N_s / k_{tw} \cdot k_{pb}} = 0.885\ \text{mm}\ /3.033 = 0.292\ \text{mm} \Rightarrow \#\,24 \Rightarrow r_{cw} = 0.288\ \text{mm} \Rightarrow$$

r_{bw}' = (0.288 mm)·(3.033) = 0.874 mm ⇒ h_{wp} = 4·r_{bw}' = 3.49 mm ⇒ tape spacing = 0.11 mm ≈ 4.3 mils

$$\text{bundle twist pitch} = p = 30 \cdot (0.885\ \text{mm} - 0.288\ \text{mm}) = 30 \cdot (0.597\ \text{mm}) = 18\ \text{mm}$$

Bundle packing of seven strands is improved slightly over five strands. Because of tighter packing,

$$\text{primary } I_{\max} = 2 \cdot [7 \cdot I_{\max}(\#\,24)] = 14 \cdot (0.94\ \text{A}) = 13.16\ \text{A} \Rightarrow$$

$$\text{max } \tilde{i}_p = (\tilde{J} / \tilde{J}_0) \cdot I_{\max} = (0.978) \cdot (13.16\ \text{A}) = \mathbf{12.87\ A} \Rightarrow I_g = (1.633) \cdot \tilde{i}_p = (1.633) \cdot (12.87\ \text{A}) = \mathbf{21.0\ A}$$

$$\overline{P}_{g0} = V_{g\min} \cdot I_g = \mathbf{420\ W} < \overline{P}_{g0}(\max) = 457\ \text{W}$$

$$R_{wpopt} = \frac{\psi \cdot \overline{P}_c / 4}{\tilde{i}_p^{\,2}} = \frac{0.476\,\text{W}}{\tilde{i}_p^{\,2}} \approx \frac{0.476\,\text{W}}{(21.0\,\text{A})^2} = 1.08\,\text{m}\Omega$$

$$\text{Per-layer bundle } f_{ropt} = 2 \cdot R_{wpopt} / R_{\delta r} = 2 \cdot (1.08\ \text{m}\Omega / 33.0\ \text{m}\Omega) = 0.065$$

The twisted seven-strand bundle has the Dowell-equation (Fig. 3) eddy-current effect for 2.65 layers (an average of M_{sb} and M_{sh}) of #24 wire. The resistance ratio from Fig. 3, for #24 wire with 2.65 layers is F_r(# 24, 2.65) ≈ 4.2. For parallel bundles, f_r = 4.2/14 = 0.30. In addition, the bundle skin-effect for two parallel bundles from the skin-effect equation is

$$f_{rSb} = F_{rw}(\text{bundle})/2 = F_{rw}(r_c \cdot \sqrt{N_s})/2 = F_{rw}\{(0.258\text{ mm})\cdot(2.646)\}/2 = F_{rw}(0.683\text{ mm})/2$$

$$= F_{rw}(\text{AWG} - 10\cdot\log(N_s))/2 = F_{rw}(24 - 8.45)/2 = F_{rw}(\#\,15.55)/2 = 0.25/2 = 0.125 \Rightarrow$$

$$f_r = f_r(\#\,24, 2.65) + F_{rw}(\#\,15.55)/2 = 0.30 + 0.125 = 0.425 = 6.54\cdot f_{ropt} = (6.54)\cdot(0.065)$$

For $f_{ropt} = f_r = 0.425$, working backwards, $R_{wopt} = 7.013$ mΩ, $\tilde{i}_p = 8.24$ A, and $\overline{P}_{g0} = 269$ W. The seven-strand plan is

2 primary windings of 6 turns each of 2 parallel layers of twisted # 23 × 7 with twist pitch p = 18 mm

Seven-strand eddy-current loss exceeds f_{ropt} by × 6.54. The bundle skin-effect is being applied to two-layer bundles with center strands shorter than the six outer strands. Consequently, the center strand will conduct more static current, offsetting the bundle skin-effect outer layer current, and the f_{rSb} calculation is probably high. Even so, the seven-strand plan must reduce power to meet the thermal requirement and desired positioning of η_{max} within the current range.

Plan E: Eight-Strand Multifilar Bundle

The two primary windings have four strands each with both windings sharing half of the multifilar strands. The multifilar bundle has twice the diameter of previous 6 × 2 half-width windings and forms a 6 × 1 configuration across the entire primary winding area.

Multifilar bundling increases coupling between primary windings and reduces leakage-inductance power loss in the primary RC clamp. With more strands in the bundle, intrabundle eddy-current loss seems like it should be greater, but in a BPP transfer circuit during on-time, both windings conduct and their fluxes cancel while during off-time, only half of the strands are conducting or else briefly are canceling. Thus, the multifilar scheme apparently has advantages over the Fig. 6 design.

Bifilar plan E combines strands of the two primary windings into a single bundle of six turns in one layer. Then fitting by width,

$$r_{bw}' = \tfrac{1}{2}\cdot(20.9\text{ mm})/6 = 1.742\text{ mm}$$

To contrast how a choice of strands affects input power, eight strands are chosen first and with each primary winding conducting separately (or in flux cancellation), the magnetic $N_s = 4$. They configure into a nested square with twisted bundle radius 3.773 × strand radius;

$$r_{cw} = r_{bw}'/\sqrt{N_s/k_{tw}\cdot k_{pb}} \approx 1.742\text{ mm}/3.773 = 0.462\text{ mm} \Rightarrow \#\,20 \Rightarrow r_{cw} = 0.448\text{ mm} \Rightarrow$$

$$r_{bw}'(\#20) = r_{cw}\cdot\sqrt{N_s/k_{tw}\cdot k_{pb}} = (0.448\text{ mm})\cdot(3.773) = 1.690\text{ mm} \Rightarrow p = 30\cdot(1.690\text{ mm}) = 50.7\text{ mm}$$

The winding height is

$$h_{wp} = 2\cdot(1.69\text{ mm}) = 3.38\text{ mm} = (0.94)\cdot(3.6\text{ mm}) \Rightarrow \text{tape spacing} = 0.22\text{ mm} = 8.7\text{ mils}$$

Ampacity and transfer power per winding is

$$\text{primary } I_{max} = 4\cdot I_{max}(\#\,20) = 4\cdot(2.369\text{ A}) = 9.48\text{ A} \Rightarrow \max \tilde{i}_p = (\tilde{J}/\tilde{J}_0)\cdot I_{max} = (0.978)\cdot(9.48\text{ A}) = \mathbf{9.27\ A} \Rightarrow$$

$$\max I_g = (1.633)\cdot\tilde{i}_p = (1.633)\cdot(9.27\text{ A}) = \mathbf{15.1\ A}$$

$$\overline{P}_{g0} = V_{g\min} \cdot I_g = (20\ \text{V}) \cdot (15.1\ \text{A}) = \mathbf{302\ W} << \overline{P}_{g0}(\max) = 457\ \text{W}$$

$$R_{wpopt} = \frac{\psi \cdot \overline{P}_c / 4}{\tilde{i}_p^{\,2}} = \frac{0.476\,\text{W}}{\tilde{i}_p^{\,2}} \approx \frac{0.476\,\text{W}}{(15.1\,\text{A})^2} = 2.09\,\text{m}\Omega$$

From R_{wpopt} calculate the eddy-current bundle resistance-ratio goal f_{ropt} for each of two parallel bundles:

$$R_{\delta r} = 33.0\ \text{m}\Omega \Rightarrow f_{ropt} = 2 \cdot R_{wpopt} / R_{\delta r} = 2 \cdot (0.063) = 0.127$$

Four twisted strands have only strand skin-effect with F_{rw}(#20), read from Fig. 3:

$$f_r = f_{rSs} = F_{rw}(\#20)/4 = 0.50/4 = 0.125 \approx f_{ropt} = 0.127$$

The four-strand eddy-current loss meets the f_{ropt} goal but input power (302 W) is low. The eight-strand multifilar plan specification is

Multifilar primary windings of 6 turns of one layer of twisted # 20 × 8 with twist pitch p = 50.7 mm

Plan F: Six-Strand Multifilar Bundle

Now choose six strands—three per primary winding. Six strands can form either a hexagonal or triangular configuration. If the result while winding is random, then an average for the twisted bundle radius-to-strand radius is 2.785.[17]

$$r_{cw} = r_{bw}' / \sqrt{N_s / k_{tw} \cdot k_{pb}} \approx 1.742\ \text{mm}/2.785 = 0.625\ \text{mm} \Rightarrow \#\,17 \Rightarrow r_{cw} = 0.625\ \text{mm} \Rightarrow$$

$$r_{bw}'(\#17) = r_{cw} \cdot \sqrt{N_s / k_{tw} \cdot k_{pb}} = (0.625\ \text{mm}) \cdot (2.785) = 1.742\ \text{mm} \Rightarrow p = 30 \cdot (1.742\ \text{mm}) = 52.3\ \text{mm}$$

For a bundle of twisted #17 × 6 strands,

$$h_{wp} = 2 \cdot (1.742\ \text{mm}) = 3.484\ \text{mm} = (0.97) \cdot (3.6\ \text{mm}) \Rightarrow \text{tape spacing} = 0.11\ \text{mm} = 4.25\ \text{mils}$$

Ampacity and power are

$$\text{primary } I_{\max} = 3 \cdot I_{\max}(\#\,17) = 3 \cdot (4.738\ \text{A}) = 14.21\ \text{A} \Rightarrow \max\ \tilde{i}_p = (\tilde{J} / \tilde{J}_0) \cdot I_{\max} = (0.978) \cdot (14.21\ \text{A}) = \mathbf{13.9\ A} \Rightarrow$$

$$\max I_g = (1.633) \cdot \tilde{i}_p = (1.633) \cdot (13.9\ \text{A}) = \mathbf{22.7\ A}$$

$$\overline{P}_{g0} = V_{g\min} \cdot I_g = (20\ \text{V}) \cdot (22.7\ \text{A}) = \mathbf{454\ W} \approx \overline{P}_{g0}(\max) = 457\ \text{W}$$

The six-strand bundle of three strands per winding has greater current density than for eight strands and has an input power close to the ideal maximum. For maximum power transfer the resistance goal for each primary winding is

$$R_{wpopt} = \frac{\psi \cdot \overline{P}_c / 4}{\tilde{i}_p^{\,2}} = \frac{0.476\,\text{W}}{\tilde{i}_p^{\,2}} \approx \frac{0.476\,\text{W}}{(13.9\,\text{A})^2} = 2.464\,\text{m}\Omega$$

From R_{wpopt} calculate the eddy-current bundle resistance-ratio goal f_{ropt}:

$$R_{\delta r} = 33.0\ \text{m}\Omega \Rightarrow f_{ropt} = R_{wpopt}/R_{\delta r} = 2.464\ \text{m}\Omega/33\ \text{m}\Omega = 0.075$$

Each twisted pair of three-strand bundles has only strand skin-effect with F_{rw}(#17), read from Fig. 3:

$$f_r = f_{rSs} = F_{rw}(\#17)/3 = 0.30/3 = 0.10 > f_{ropt} = 0.075$$

The three-strand eddy-current loss exceeds f_{ropt} by × 1.33 but power is near maximum. The six-strand plan specification is

Multifilar primary windings of 6 turns each of one layer of twisted # 17 × 6 with twist pitch p = 52.3 mm

The eight-strand plan E has lower winding loss only because it is has less current density and provides only ⅔ the input power of the six-strand plan. The six-strand scheme has $f_r = f_{ropt}$ at $\tilde{i}_p$ = 12.0 A and 392 W. The excess of f_r is small (33%) and plan F provides the most transfer power.

Comparing Different Bundle Plans

The calculated plans for ETD34 dual primary windings are summarized in the table.

Table. Alternative plans for ETD34 primary windings.

Plan	N_s	Bundling	r_{cw}, AWG	$\tilde{i}_p$, A	I_g, A	$\overline{P}_{g0}$, W	f_{ropt}	f_r	f_r/f_{ropt}
A	3	2 || bundles	20	13.91	22.7	454	0.075	0.083	0.90
B	4	2 || bundles	23	9.26	15.1	302	0.127	0.22	1.73
C	5	2 || bundles	23	11.58	18.9	378	0.081	0.176	2.17
D	7	2 || bundles	24	12.87	21.0	420	0.065	0.185	2.85
E	4 × 2	multifilar	20	9.27	15.1	302	0.127	0.125	0.98
F	3 × 2	multifilar	17	13.9	22.7	454	0.075	0.10	1.33

Closest to achieving the design goals are plans A and F. Plan A comes closest to the f_r and $\overline{P}_{g0}$ goals. Plan F comes closest after plan A to achieving $\overline{P}_{g0}(\max)$ but its f_r and winding resistance are higher. However, being multifilar wound, loss of primary-winding leakage energy and circuit resonance are less, possibly offsetting greater winding loss.

Except for plans A and F, the only other plan that is close to the $\overline{P}_{g0}$ goal is plan D. Its transfer power is low because strand packing and hence current density is lower than in plan F.

Plans A through D and Plans E and F have within them a given bundle size or area in which different numbers of strands are tried. The overall goal in maximizing transfer power is to maximize current density in the given winding area while constraining f_r. Winding dimensions for high-current windings have a dominating effect on plan performance. Plan F is chosen for the Volksinverter.

However, the other plans have some relevance to existing designs. Plan D can be compared to the Statpower 500 inverter. It has a push-pull (PP) transfer circuit with the following transformer characteristics as observed from a disassembled unit:

Core: PQ32/20, V = 9.44 cm^3; primaries: 2 × twisted # 21 × 7 (13 A), p/r_{bw}' = 20, $L_p \approx$ 58.7 μH, turns ratio n = 1/3.8;

secondary: twisted #21 × 2 (3.5 A), L_s = 848 μH; 8 parallel power-transfer circuits

The Statpower 500 design is similar to a Samlex PSE-24175A with a (continuous) power rating of 1750 W or 1750 W/8 = 219 W per transformer. A photograph of the top side of the Samlex circuit-board is shown in Fig. 7. Unlike the similar design of the Statpower 500 with PQ cores, the transformers have EE or EER cores of comparable size.

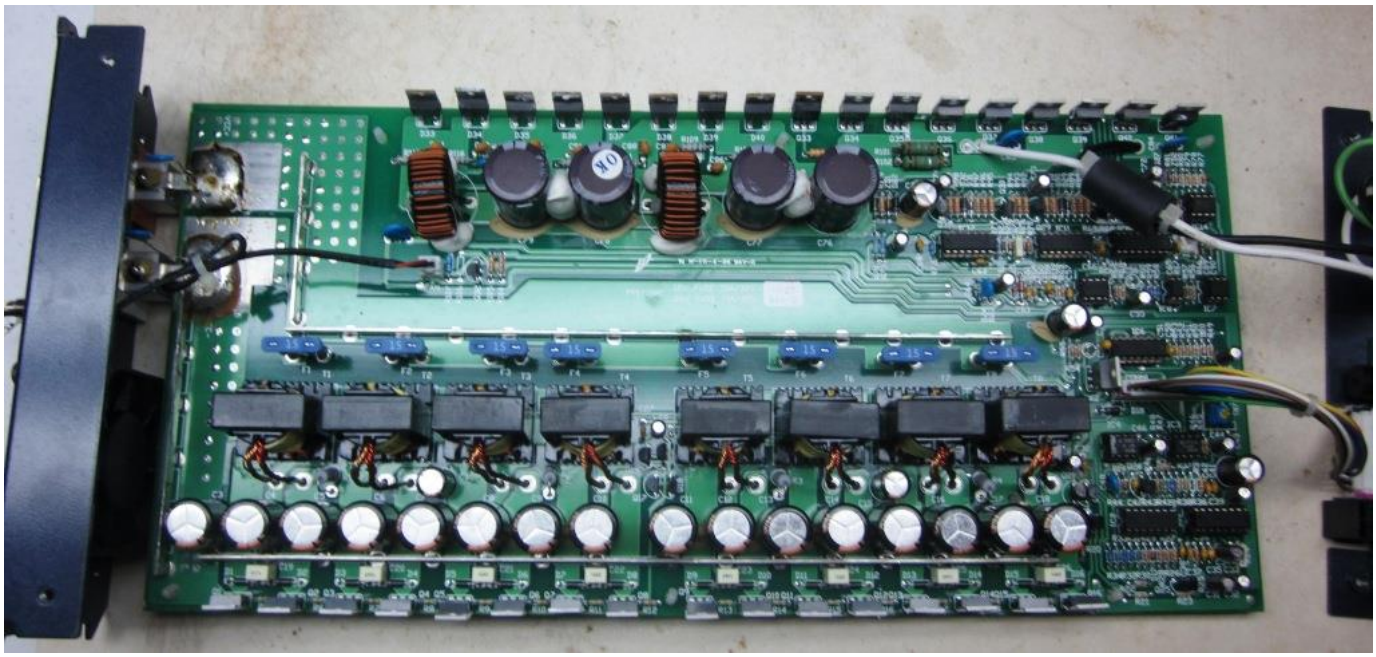

Fig. 7. Top view of the circuit-board of the Samlex PSE-24175A inverter. Eight converter transformers along the bottom half of the board sustain the rating of 1750 W of continuous power. The design is essentially a refined Statpower 500. Two toroidal inductors on the top half of the board in the secondary circuit make it a buck with a push-pull primary.

The Volksinverter ETD34 core has a magnetic volume V = 7.64 mm^3, which is about 20% smaller than the PQ32/20. The Samlex power rating is about half that of plan F. Closest in construction to the Statpower transformer design is plan D, which at the calculated f_r can sustain 269 W, about 23% more power than the Statpower rating. This offers some commercial confirmation of the design formulas and procedures given here short of converter prototype testing.

The seven-strand #21 AWG primary winding of the Statpower 500 also has a static bundle ampacity of about 13 A, comparable to the 13 A (12.97 A) calculated in part 16. The difference is that Volksinverter plan F has 454 W/219 W = 2.07 or twice the predicted transfer power. Also, the choice of 1/n = 4 compares to the Statpower 1/n = 3.8 and is between it and the Sumry 3-kW inverter choice of 1/n = 4.3. This affects the power rating of both transformer and inductor.

The Statpower 500 and Samlex PSE-24175A both have transfer circuits with push-pull primaries and buck secondaries. The series inductor on the primary side of the Volksinverter is replaced by one in the secondary circuit, converting the circuit from a CA (boost) to a CP (buck) PWM-switch configuration.

In part 14, a full-bridge buck was compared to the boost push-pull (BPP). The analysis showed the BPP to be somewhat superior. In either case, the addition of the inductor on either side improves reliability and control over push-pull chopper circuits found in low-cost, lower-power inverters.

References

Except for the last reference, which comes from the APEC 2003 proceedings, all of the following works were published in the How2Power Today newsletter in the issues indicated. However, many of the same concepts are covered in the author's power-electronics books, which are available for download at innovatia.com.

1. "Designing An Open-Source Power Inverter (Part 1): Goals And Specifications" by Dennis Feucht, How2Power Today, May 2021.
2. "Designing An Open-Source Power Inverter (Part 2): Waveshape Selection" by Dennis Feucht, How2Power Today, September 2021.
3. "Designing An Open-Source Power Inverter (Part 3): Power-Transfer Circuit Options" by Dennis Feucht, How2Power Today, April 2022.
4. "Designing An Open-Source Power Inverter (Part 4): The Optimal Power-Line Waveshape" by Dennis Feucht, How2Power Today, May 2022.
5. "Designing An Open-Source Power Inverter (Part 5): Kilowatt Inverter Circuit Design" by Dennis Feucht, How2Power Today, July 2022.
6. "Designing An Open-Source Power Inverter (Part 6): Kilowatt Inverter Control Circuits" by Dennis Feucht, How2Power Today, August 2022.
7. "Designing An Open-Source Power Inverter (Part 7): Kilowatt Inverter Magnetics" by Dennis Feucht, How2Power Today, September 2022.
8. "Designing An Open-Source Power Inverter (Part 8): Converter Control Power Supply" by Dennis Feucht, How2Power Today, November 2022.
9. "Designing An Open-Source Power Inverter (Part 9): Magnetics For The Converter Control Power Supply" by Dennis Feucht, How2Power Today, December 2022.
10. "Designing An Open-Source Power Inverter (Part 10): Converter Protection Circuits" by Dennis Feucht, How2Power Today, February 2023.
11. "Designing An Open-Source Power Inverter (Part 11): Minimizing Switch Loss In Low-Input-Resistance Converters" by Dennis Feucht, How2Power Today, March 2023.
12. "Designing An Open-Source Power Inverter (Part 12): Sizing The Converter Magnetics" by Dennis Feucht, How2Power Today, March 2023.
13. "Designing An Open-Source Power Inverter (Part 13): The Differential Boost Push-Pull Power-Transfer Circuit" by Dennis Feucht, How2Power Today, June 2023.
14. "Designing An Open-Source Power Inverter (Part 14): Boost Push-Pull Or Buck Bridge?" by Dennis Feucht, How2Power Today, July 2023
15. "Designing An Open-Source Power Inverter (Part 15): Transformer Magnetic Design For the Battery Converter" by Dennis Feucht, How2Power Today, March 2024.
16. "Designing An Open-Source Power Inverter (Part 16): Transformer Winding Design For the Battery Converter—Efficiency Range And Winding Allotment" by Dennis Feucht, How2Power Today, April 2024.
17. "The Geometry of Twisted Wire Bundles" by Dennis Feucht, How2Power Today, July 2018.
18. "How Twisted Bundles Reduce Eddy-Current Effects In Winding Bundle Design" by Dennis Feucht, How2Power Today, September 2023.
19. "Magnetizing Current and Transformer Design Optimization" by Dennis Feucht, How2Power Today, October 2023.
20. "How Wire Bundle Configurations Influence Eddy-Current Proximity Effects" by Dennis Feucht, How2Power Today, February 2019.
21. "Bundle Compression Overcomes Aspect Ratio Constraints On Transformer Design," by Dennis Feucht, How2Power Today, June 2018.

22. "Optimal Core Dimensional Ratios for Minimizing Winding Loss in High-Frequency Gapped-Inductor Windings" by R. Jensen and C. R. Sullivan, *IEEE Applied Power Electronics Conference*, FEB03, pp. 1164-1169.

About The Author

Dennis Feucht has been involved in power electronics for 40 years, designing motor-drives and power converters. He has an instrument background from Tektronix, where he designed test and measurement equipment and did research in Tek Labs. He has lately been working on projects in theoretical magnetics and power converter research.

For more on magnetics design, see these How2Power Design Guide search results.

Appendix: Innovatia Wire Table

The following wire table is used at Innovatia Laboratories. These notes apply to terminology used in this table:

Cu ampacity I (AWG) = 4.5 A/mm^2·A_c(AWG); A_{cw}(AWG) = π·r_{cw}^2

Wire packing factor k_p = k_{pf} · k_{pw}, k_{pw} = wire porosity = A /A_{cw}

Fill factor $k_{pf} = \frac{7}{8}\cdot\frac{\pi}{2\cdot\sqrt{3}} \approx \frac{1}{1.260}$ $A_{cwp}(AWG) = \frac{A_{cw}(AWG)}{k_{pf}} = \frac{A_c}{k_p}$ $A_c(AWG) = (53.48\,\text{mm}^2)\cdot 10^{\frac{-AWG}{9.97}}$

Frequency at which wire radius r_c equals skin depth δ in Hz:

$$f_\delta = \left(\frac{73.5\,\text{mm}}{r_c}\right)^2 \cdot \text{Hz}, \text{Cu}, 80\,^\circ\text{C} \qquad f_\delta = \left(\frac{94\,\text{mm}}{r_c}\right)^2 \cdot \text{Hz}, \text{Al}, 80\,^\circ\text{C}$$

Innovatia wire table. (heavy (double) insulation r_c: 20 AWG/dec ≈ 6 AWG/oct; A_c:10 AWG/dec ≈ 3 AWG, f_δ @ 80°C).

Gage, AWG	r_c, mm	r_{cw}, mm	A_c, mm^2	A_{cwp}, mm^2	k_p	I_{max}, A	$f_{\delta Cu}$, kHz	$f_{\delta Al}$, kHz
0	4.126	4.251	53.482	71.552	0.747	240.67	0.317	0.519
1	3.676	3.794	42.449	56.987	0.745	191.019	0.400	0.655
2	3.275	3.023	33.692	45.395	0.742	151.612	0.505	0.826
3	2.918	2.986	26.741	36.169	0.739	120.335	0.636	1.041
4	2.599	2.698	21.224	28.824	0.736	95.510	0.802	1.312
5	2.316	2.409	16.846	22.976	0.733	75.806	1.012	1.656
6	2.063	2.151	13.371	18.318	0.730	60.167	1.276	2.086
7	1.838	1.921	10.612	14.608	0.726	47.755	1.608	2.630
8	1.637	1.716	8.423	11.653	0.723	37.903	2.028	3.318
9	1.459	1.533	6.685	9.298	0.719	30.084	2.559	4.185
10	1.300	1.369	5.306	7.421	0.715	23.877	3.226	5.277
11	1.158	1.223	4.211	5.925	0.711	18.952	4.071	6.658
12	1.032	1.093	3.343	4.732	0.706	15.042	5.132	8.394
13	0.919	0.977	2.653	3.780	0.702	11.939	6.453	10.554
14	0.819	0.874	2.106	3.021	0.697	9.476	8.153	13.335
15	0.729	0.781	1.671	2.415	0.692	7.521	10.278	16.810
16	0.650	0.698	1.327	1.931	0.687	5.969	12.985	21.239
17	0.579	0.625	1.053	1.545	0.681	4.738	16.340	26.725
18	0.516	0.559	0.836	1.237	0.670	3.760	20.608	29.668
19	0.459	0.500	0.663	0.990	0.671	2.985	25.980	42.494
20	0.409	0.448	0.526	0.793	0.664	2.369	32.613	53.342
21	0.365	0.401	0.418	0.636	0.657	1.880	41.225	67.428
22	0.325	0.359	0.332	0.510	0.651	1.492	52.103	85.220
23	0.289	0.321	0.263	0.409	0.644	1.184	65.586	107.27
24	0.258	0.288	0.288	0.328	0.637	0.940	82.432	134.83
25	0.230	0.258	0.166	0.264	0.629	0.746	103.92	169.98
26	0.205	0.231	0.132	0.212	0.622	0.592	132.40	216.55
27	0.182	0.207	0.104	0.170	0.614	0.470	164.90	269.71
28	0.162	0.186	0.083	0.137	0.605	0.373	211.03	345.16
29	0.145	0.167	0.066	0.110	0.597	0.296	260.53	426.12
30	0.129	0.150	0.052	0.089	0.588	0.235	334.94	547.83
31	0.115	0.134	0.041	0.072	0.579	0.187	423.08	691.99
32	0.102	0.121	0.033	0.058	0.570	0.148	519.25	849.29
33	0.091	0.108	0.026	0.047	0.561	0.118	666.94	1091
34	0.081	0.097	0.021	0.038	0.551	0.093	844.10	1381
35	0.072	0.088	0.016	0.030	0.541	0.074	1072	1753
36	0.064	0.079	0.013	0.025	0.531	0.059	1148	2157
37	0.057	0.071	0.010	0.020	0.521	0.047	1663	2720
38	0.051	0.064	0.00823	0.016	0.511	0.037	2077	3397
39	0.046	0.057	0.00653	0.013	0.500	0.029	2668	4364
40	0.041	0.052	0.00518	0.011	0.489	0.023	3376	5523
41	0.036	0.047	0.00411	0.0086	0.479	0.019	4168	6818
42	0.032	0.042	0.00326	0.0070	0.467	0.015	5276	8629
	0.892		2.5	3-wire cable		11.25	6.79	
	1.128		4.0			18.0	4.24	
12.7 mm × 76.3 µm (0.5 in., 3 mil) Cu foil			0.968			4.36	928	1518